

# Accessing Semi-Addressable Self Assembly with Efficient Structure Enumeration

Maximilian C. Hübl\* and Carl P. Goodrich†

*Institute of Science and Technology Austria (ISTA), Am Campus 1, 3400 Klosterneuburg, Austria*

(Dated: May 24, 2024)

Modern experimental methods enable the creation of self-assembly building blocks with tunable interactions, but optimally exploiting this tunability for the self-assembly of desired structures remains an important challenge. Many studies of this inverse problem start with the so-called fully-addressable limit, where every particle in a target structure is different. This leads to clear design principles that often result in high assembly yield, but it is not a scaleable approach – at some point, one must grapple with “reusing” building blocks, which lowers the degree of addressability and may cause a multitude of off-target structures to form. While the existence of off-target structures does not necessarily preclude high yield assembly of the target structure(s), it massively complicates the design process because it is often unclear if or how these off-target structures can be controlled. Here, we solve a key obstacle preventing robust inverse design in the “semi-addressable regime” by developing a highly efficient algorithm that enumerates all structures that can be formed from a given set of building blocks. By combining this with established partition-function-based yield calculations, we successfully inverse design for target structures while minimizing the required number of distinct building block species. Furthermore, we show that it is almost always possible to find semi-addressable designs where the entropic gain from reusing building blocks outweighs the presence of off-target structures and even increases the yield of the target. Thus, not only does our enumeration algorithm enable robust and scalable inverse design in the semi-addressable regime, our results demonstrate that it is possible to operate in this regime while maintaining the level of control often associated with full addressability.

Keywords: inverse self assembly | semi-addressable regime | structure enumeration | reverse search

The so-called fully-addressable limit, where every particle in a target structure is different and individually tunable, is a central paradigm in inverse self assembly [1–8]. It leads to clear design principles for particle-particle interactions that prevent uncontrolled aggregation and allow the targeting of complex, precisely defined structures. However, making every particle different is not scalable, as it couples (experimental) cost and complexity to the size and number of desired structures. To overcome this, one must venture away from the fully-addressable limit and into what we call the *semi-addressable regime* (Fig. 1), where binding is no longer deterministic and building blocks can fit together in more than one way.

In contrast to fully-addressable assembly, there exists an enormous number of semi-addressable designs for a given target, and most of these designs also lead to a large number of off-target structures that lower the chance of successful assembly. On the other hand, reusing the same particle species multiple times in the same structure raises the structure’s configurational entropy [9, 10], which positively affects its yield. Does this mean that it is possible to find semi-addressable designs with high target yields in spite of many off-target structures? Identifying such designs is a considerable challenge, as it is not enough to design *for* a target structure, one must simultaneously design *against* all the off-targets. Nevertheless, there is a path forward: if all competing struc-

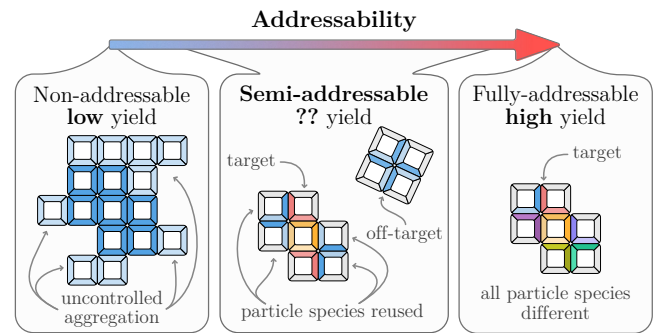


FIG. 1. Different degrees of addressability. Non-addressable building blocks lead to uncontrolled aggregation, while a precise target shape can be encoded with fully addressable building blocks. Depending on the degree of addressability, semi-addressable designs lead to varying numbers of competing structures, whose impact on yield is often hard to predict.

tures are known, equilibrium yields can be efficiently predicted through an established partition-function-based approach [11–14]. In many cases, this calculation is fast enough that one could iterate over the discrete binding rules (*e.g.* using the approach of Ref. [15]) and thus perform inverse design. The bottleneck, however, is actually enumerating all the relevant off-target structures, the number of which can change by many orders of magnitude with very slight changes to the binding rules.

In this paper, we overcome this major obstacle by introducing a general and highly efficient algorithm for enumerating self-assembled structures. This algorithm operates on minimal assumptions and can be used in most

\* maximilian.huebl@ist.ac.at

† carl.goodrich@ist.ac.at

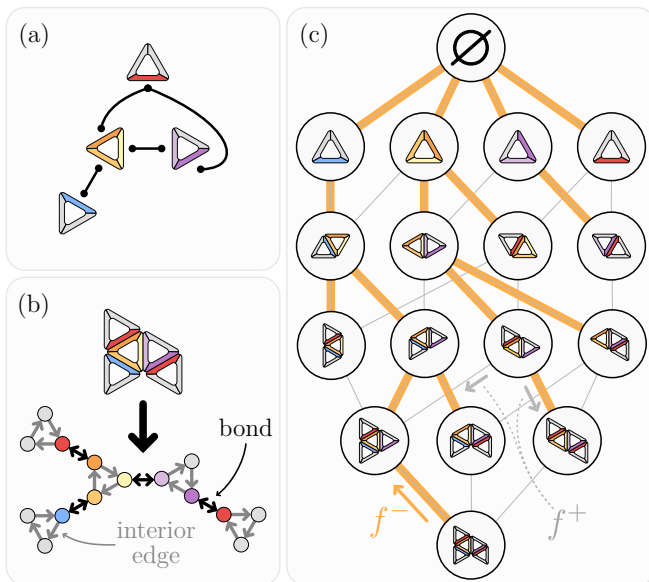


FIG. 2. Reverse search enumeration. (a) Diagrammatic representation of an assembly system consisting of 4 triangular building blocks with potential binding sites on the triangle edges. Two edges can bind only if they are connected in the diagram. Sites without connections are inert and are shown in grey. (b) A structure and its anatomy, *i.e.* its associated vertex-colored, directed graph. (c) The 16 structures resulting from the assembly system in (a), together with the empty structure  $\emptyset$ , form a structure graph. Reverse search uses the functions  $f^+(s)$  and  $f^-(s)$ , which depend on the anatomy, to construct a spanning tree (orange lines), that can be traversed efficiently.

experimental or computational settings. We then show how this algorithm enables robust inverse design in the semi-addressable regime by combining it with partition-function-based yield calculations to identify nontrivial interaction patterns that maximize the yield of desired structures. Contrary to the natural expectation that off-target structures necessarily hurt the assembly of the target, we show that there almost always exists a semi-addressable design where this is overcome by the entropic benefits of fewer species, leading to better yields compared to the fully-addressable limit even when there are many off-target structures. This result means that yield does not have to be compromised to satisfy experimental constraints or to access other benefits of the semi-addressable regime (*e.g.* designing reconfigurable structures, hierarchical structures [9, 16, 17], or multiple structures in parallel [18–20]).

We begin by defining an *assembly system* as a set of building block species and binding rules, as exemplified in Fig. 2a. We assume that building blocks interact through discrete, orientationally-locking bonds. Such interactions ensure that a structure’s topology cannot change through large deformations, and are common in many self-assembling systems, such as the assembly of DNA-Origami particles [21–24], DNA-bricks [7, 8, 25] or

certain types of *de novo* proteins [26, 27]. Given an assembly system and optional constraints (*e.g.* maximum structure size), we use reverse search [28–30] together with a graph-encoding of structures to efficiently enumerate the set of all structures  $\mathcal{S}$  that can be formed by connecting building blocks site-to-site.

Reverse search is a general enumeration procedure that can be applied to a wide range of enumeration or search problems, and guarantees a runtime linearly proportional to the size of the output [28]. To apply reverse search, we first need two functions: a ‘raise’ function  $f^+(s)$  that returns all structures that can be created by concatenating a building block onto a pre-existing structure  $s$ , and a ‘lower’ function  $f^-(s)$  that removes a building block from  $s$ . Note that while the raise function  $f^+(s)$  returns an ordered list of structures  $[f^+(s)]_i$ , the lower function  $f^-(s)$  *arbitrarily but deterministically* returns a single structure. The challenge here is making these two functions well-defined, so that their output only depends on the topology of the input structure, and not on the way the structure is represented in memory. We solve this by encoding structures as vertex-colored directed graphs, called the *anatomy* (Fig. 2b), which allows us to define  $f^+(s)$  and  $f^-(s)$  using graph-theoretical tools, as explained below.

Given these functions, reverse search works by generating structures through  $f^+(s)$  and then filtering them through  $f^-(s)$  [28]. Starting from the empty structure  $s = \emptyset$ , we use  $f^+(s)$  to generate offspring  $u_i = [f^+(s)]_i$ , but only accept those offspring that lead back to  $s$  after lowering them, *i.e.* only those  $u_i$  for which  $f^-(u_i) = s$ , as shown in Fig. 2c. This process is repeated for all accepted offspring until no new offspring are found. The memory requirement of this enumeration procedure is independent of the number of structures  $N_{\text{str}} = |\mathcal{S}|$ , and the time complexity is  $O(ztN_{\text{str}})$ , where  $z$  is the maximum number of offspring and  $t$  is the time to evaluate  $f^+(s)$  and  $f^-(s)$  [28].

To implement  $f^+(s)$  and  $f^-(s)$  and to check structures for equality, we encode a structure  $s$  as a vertex-colored directed graph, which we call the structure anatomy  $a(s)$ . The binding sites of  $s$  correspond to the vertices of  $a(s)$ , which are colored according to the type of binding site. There are two types of edges in  $a(s)$ : first, all bonds between building blocks correspond to double-ended edges between the bound sites. Second, the sites of each building block are connected with ‘interior’ edges that encode the building block geometry. Interior edges and vertex colorings of  $a(s)$  can be implemented in multiple ways, but if building blocks are symmetric, care must be taken to ensure that the automorphism group of  $a(s)$  is isomorphic to the symmetry group of  $s$  (see SI). In two dimensions, this can be achieved by simply encoding building blocks as oriented cycles, as shown in Fig. 2b.

The structure anatomy allows us to define  $f^+(s)$  and  $f^-(s)$  through a graph-theoretic procedure known as *canonical labeling* [31, 32], which is a special labeling of a graph’s vertices with the property that two graphs have

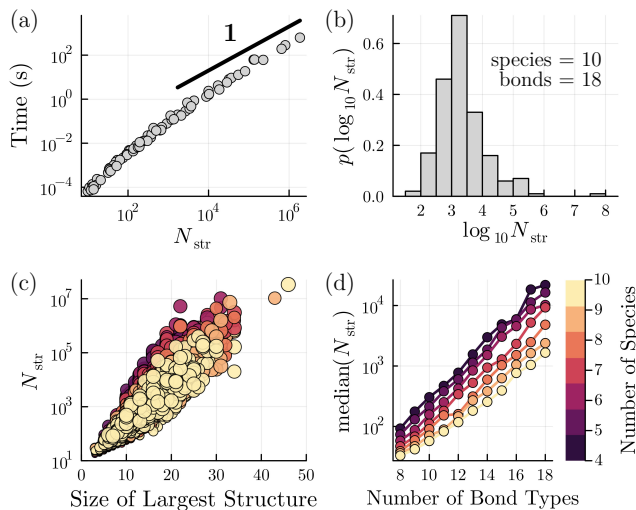


FIG. 3. Algorithm performance and assembly system statistics. (a) Runtime of the enumeration algorithm for different number of structures  $N_{\text{str}}$ . The tested systems consist of randomly generated systems as well as single-species triangular polyforms up to size 17. The benchmark was performed on a single 2.3 GHz core of a 2019 MacBook Pro. The black line with slope 1 is a guide to the eye and corresponds to the theoretical large- $N_{\text{str}}$  scaling. (b) Histogram of the logarithm of  $N_{\text{str}}$  for 10 species and 18 bond types. (c) The total number of structures  $N_{\text{str}}$  as a function of size of the largest structure. Data is colored by the number of building block species and the marker size is proportional to the number of bond types. (d) Median number of structures  $\text{median}(N_{\text{str}})$  as a function of the number of bonds types for different numbers of species.

identical canonical labelings if and only if they are isomorphic. In our case, we exploit the canonical labeling of the anatomy  $a(s)$  to define a unique and deterministic ordering of a structure’s binding sites that does not depend on the order in which its particles were connected together. We then define  $f^-(s)$  to remove the particle that contains the site with the highest canonical label and whose removal does not disconnect the structure. Similarly,  $f^+(s)$  can be defined by ordering a structure’s binding sites and all compatible building block species, iterating through the possible pairs of binding sites and species and finally rejecting concatenations if they lead to particle overlap or violate an imposed constraint (see SI). We also use canonical labeling to compare structures for equality, as two structures are identical if and only if their canonically labeled anatomies are identical. While generating canonical labels is a difficult problem in general, in practice we employ *nauty* [32], which can canonize the type of graphs we encounter here in a few microseconds [33]. A measure of the real-world performance of our implementation of the algorithm [34] is shown in Fig. 3a.

A key strength of our approach is that it is easily adapted to any system with orientationally locking interactions, as our algorithm decouples the low-level enu-

meration procedure from the physics and geometry of the building blocks. In contrast to other applications of reverse search to structure enumeration problems [35, 36], our graph-encoding technique allows our algorithm to work off-lattice, handle multiple species, and incorporate binding rules and constraints. For us, all that is needed to define a particular building block are the locations and orientations of its binding sites, its symmetry group and a function that determines when two building blocks overlap (see SI). Building blocks that tile space or are convex can lead to performance gains, but are not required. We verified that our algorithm works as expected by reproducing known numbers of different 2D and 3D polyforms as shown in the SI.

As a first application of our procedure, we ask whether the number of structures  $N_{\text{str}}$  can be estimated from the number of species and/or bond types. To address this, we randomly generate assembly systems that are composed of  $N_{\text{spc}}$  species and  $N_{\text{bnd}}$  bonds. For simplicity, we reject systems that lead to infinitely many structures or allow closed structures to form (see SI), and sample 200 assembly systems for every combination of  $4 \leq N_{\text{spc}} \leq 10$  and  $8 \leq N_{\text{bnd}} \leq 18$ , as shown in Fig. 3b-d. We find that for fixed  $N_{\text{spc}}$  and  $N_{\text{bnd}}$ , the distribution of  $N_{\text{str}}$  is very long-tailed (Fig. 3b), indicating that the topology of the binding rules is critical in determining the enumeration outcome. However, some trends are evident. First, the total number of structures  $N_{\text{str}}$  is strongly correlated with the size of the largest structure in the enumeration (Fig. 3c). Additionally,  $N_{\text{str}}$  increases roughly exponentially with  $N_{\text{bnd}}$ , and it decreases with  $N_{\text{spc}}$  if the number of bonds is held fixed (Fig. 3d). Thus, while it is difficult to predict the number of structures from the basic properties of the assembly system, it can be best estimated from the number of bond types.

Finally, we return to the problem of semi-addressable inverse design. Here, it is our goal to find economical assembly systems with as few building block species as possible that can still assemble a given target structure shape at high yield. We start by considering three example target shapes: a 7-particle symmetric shape (Fig. 4a), an 8-particle asymmetric shape (Fig. 4b), and a 9-particle tree-like shape (Fig. 4c). For each shape, we perform a quasi-brute-force search [37] over assembly systems to identify the design with the highest yield of the target shape at fixed  $N_{\text{spc}}$ . To do this, we begin from the fully-addressable assembly system corresponding to the target shape and then recursively merge building block species with each other, thereby generating simpler and simpler assembly systems that still allow the target to assemble (see SI). For convenience, we reject designs that allow more than  $N_{\text{ctf}} = 2000$  different structures to form. Once all assembly systems that satisfy our constraints are found, we generate all structures of all systems.

The complete enumeration then allows us to compute equilibrium structure yields via the methods outlined in Refs. [12–14]. Briefly, the yield of a structure  $s$  is  $Y_s = \rho_s / \sum_{s' \in \mathcal{S}} \rho_{s'}$ , where  $\rho_s$  is the equilibrium number

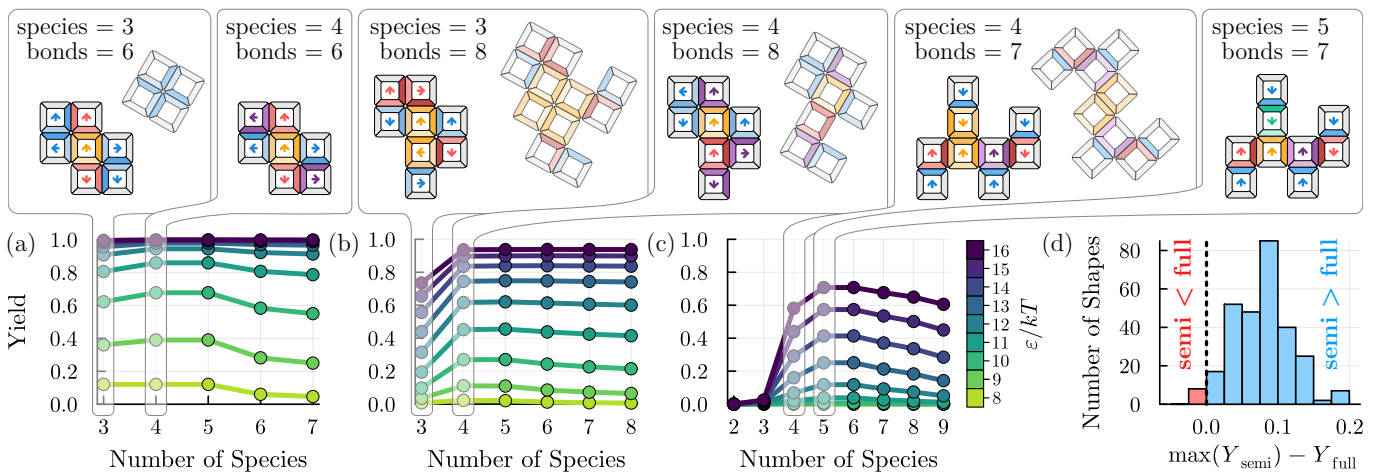


FIG. 4. Inverse design in the semi-addressable regime. For a given target shape containing (a) 7, (b) 8, and (c) 9 particles, we identify designs with a specified number of species that maximize equilibrium yield, which is shown at different binding energies  $\varepsilon$  and volume fraction  $\phi = 0.2$ . Only the highest-yield system for each species number are shown. The systems with maximal number of species are fully addressable. Colored target shapes and some competing structures (greyed out) are shown for select systems, the arrows indicate the building block orientation. (d) Histogram of the difference between the maximal semi-addressable yield  $\max(Y_{\text{semi}})$  and the fully-addressable yield  $Y_{\text{full}}$  for all square shapes of size  $1 < n < 8$ . Semi-addressable assembly improves the yield for 276 out of 284 structures (blue), whereas the yield of the 8 other structures degrades slightly (red). Yields are computed at  $\varepsilon = 14 kT$  and  $\phi = 0.2$ .

density

$$\rho_s(\mu_\alpha, \varepsilon) = \frac{A_s}{\sigma_s} e^{\beta[\sum_\alpha n_s^\alpha \mu_\alpha + k_s \varepsilon]}, \quad (1)$$

$\beta = 1/kT$  is the inverse temperature,  $\mu_\alpha$  is the chemical potential of building block species  $\alpha$ ,  $\varepsilon$  is the binding energy (which is assumed here to be the same for all bonds),  $n_s^\alpha$  is the number of building blocks of species  $\alpha$  in  $s$ ,  $k_s$  is the number of bonds in  $s$  and  $\sigma_s$  is the symmetry number of  $s$ .  $A_s$  is a prefactor that is related to the rotational and vibrational entropy of  $s$ , and depends on the details of the binding interactions. We ignore this prefactor in our initial search but include it (derived from a simple binding model, see SI) when reporting final yields in Fig. 4. Chemical potentials  $\mu_\alpha$  are chosen to correspond to stoichiometric concentrations with total particle volume fraction  $\phi = 0.2$ . More details on the calculations can be found in the SI.

Figure 4a-c shows the maximum yields as a function of  $N_{\text{spc}}$  and binding energy  $\varepsilon$ . For all three target structure shapes, yield either increases or stays roughly constant as we move from the fully- into the semi-addressable regime. Semi-addressable designs often exploit symmetries in the target structure (when applicable, *e.g.* Fig. 4a), but optimal designs do much more than just exploit symmetries, as the shapes in Fig. 4b-c are not symmetric but still exhibit economical high-yield solutions. In these examples, optimal solutions sometimes exploit steric repulsion between the inert (grey) sides of the building blocks to ‘protect’ open bonds, or even contain unprotected open bonds. As highlighted in Fig. 4, many of the minimal systems allow off-target structures to form, but these off-target structures only weakly affect yield.

The observed increase in yield in the semi-addressable regime is only possible because of the configurational entropy gain associated with permutations of indistinguishable particles [9, 10]. This effect competes with the presence of off-target structures, which lower yield, and it is *a priori* unclear which effect dominates. In fact, for a vast majority of semi-addressable systems, the number of competing structures is enormous and target yield becomes vanishingly small. However, our efficient enumeration and yield calculations allow us to identify semi-addressable systems where these two effects balance, or where the entropy gain even results in increased target yield.

Figure 4a-c show optimal designs for three arbitrarily chosen target structures, but our results are highly general. To demonstrate this, we performed the same calculation for all shapes composed of  $n < 8$  squares. As shown in Fig. 4d, we find that for 276 out of 284 shapes (97%), there exist semi-addressable designs that explicitly increase yield compared to the fully-addressable case. This demonstrates the generality of our results, implying that combining high yield with economy is a far-reaching and realistic design goal.

Using our structure enumeration algorithm, we have shown that both assembly economy and quality can be improved by venturing from the fully-addressable into the semi-addressable assembly regime. While other authors have found semi-addressable designs that prevent off-target structures [15, 38], for example by taking advantage of symmetries or repeated structural motifs, our results show that off-target structures do not have to be avoided to still achieve high equilibrium yield. This observation has profound implications for exploiting semi-

addressability for multifarious self assembly, where a single set of building blocks assembles into multiple target structures simultaneously [14, 15, 19], or for any use case where building blocks need to be reused. Furthermore, we are able to achieve these high-yield designs while adhering to the experimentally relevant constraints of equal binding energies and stoichiometric concentrations. Additionally optimizing over binding energies and monomer concentrations should lead to further increases in target yield [14], but is not necessary in the structures we study.

This result is enabled by our encoding of structures as vertex-colored directed graphs, which we call their anatomy. This anatomy allows us to efficiently define the functions  $f^+(s)$  and  $f^-(s)$ , which are the necessary ingredients for implementing reverse search. Together, this leads to an enumeration algorithm with minimal memory requirements that is so computationally efficient that we were able to perform inverse design through a quasi-brute-force approach (Fig. 4). Combining our fast enumeration and yield calculations with more efficient methods for generating candidate assembly systems, such as the techniques of Bohlin et al. [15], would allow semi-addressable inverse design of larger and more complex structures.

Our work is accompanied by an open-source, user-

orientated implementation of our enumeration algorithm [34] that can be used for any 2D or 3D system with orientationally locking interactions. This implementation could be further scaled up through large-scale parallelization, made possible by reverse search [29], or extended beyond orientationally-locking interactions by generalizing the raising and lowering functions, as discussed in the SI. Finally, structure enumeration can be critical for addressing a wide range of topics in self assembly beyond the scope of this work, including questions of kinetics [39–42] or hierarchy [9, 16, 17]. For example, the structure graph (Fig. 2c) could be exploited for Markov-based kinetic calculations, or hierarchical assembly schemes could be implemented by reusing high-yield output structures as building blocks for a second round of self assembly. We envision our enumeration algorithm to be a flexible tool for many such applications.

## ACKNOWLEDGMENTS

We thank Daichi Hayakawa, Thomas E. Videbæk, and W. Benjamin Rogers for important discussions, and Jérémie Palacci, Anđela Šarić, and Scott Waitukaitis for helpful comments on the manuscript. The research was supported by the Gesellschaft für Forschungsförderung Niederösterreich under project FTI23-G-011.

- 
- [1] S. Hormoz and M. P. Brenner, Design principles for self-assembly with short-range interactions, *Proceedings of the National Academy of Sciences* **108**, 5193 (2011).
  - [2] Z. Zeravcic, V. N. Manoharan, and M. P. Brenner, Size limits of self-assembled colloidal structures made using specific interactions, *Proceedings of the National Academy of Sciences* **111**, 15918 (2014).
  - [3] W. M. Jacobs and D. Frenkel, Self-Assembly of Structures with Addressable Complexity, *Journal of the American Chemical Society* **138**, 2457 (2016).
  - [4] W. M. Jacobs, A. Reinhardt, and D. Frenkel, Rational design of self-assembly pathways for complex multicomponent structures, *Proceedings of the National Academy of Sciences* **112**, 6313 (2015), 1502.01351.
  - [5] L. Cademartiri and K. J. M. Bishop, Programmable self-assembly, *Nature Materials* **14**, 2 (2015).
  - [6] L. O. Hedges, R. V. Mannige, and S. Whitlam, Growth of equilibrium structures built from a large number of distinct component types, *Soft Matter* **10**, 6404 (2014), 1405.2145.
  - [7] B. Wei, M. Dai, and P. Yin, Complex shapes self-assembled from single-stranded DNA tiles, *Nature* **485**, 623 (2012).
  - [8] Y. Ke, L. L. Ong, W. M. Shih, and P. Yin, Three-Dimensional Structures Self-Assembled from DNA Bricks, *Science* **338**, 1177 (2012).
  - [9] S. Whitlam, Hierarchical assembly may be a way to make large information-rich structures, *Soft Matter* **11**, 8225 (2015), 1505.07501.
  - [10] D. Frenkel, Order through entropy, *Nature Materials* **14**, 9 (2015).
  - [11] M. Holmes-Cerfon, Sticky-Sphere Clusters, *Annual Review of Condensed Matter Physics* **8**, 77 (2016), 1709.05138.
  - [12] A. I. Curatolo, O. Kimchi, C. P. Goodrich, R. K. Krueger, and M. P. Brenner, A computational toolbox for the assembly yield of complex and heterogeneous structures, *Nature Communications* **14**, 8328 (2023).
  - [13] E. D. Klein, R. W. Perry, and V. N. Manoharan, Physical interpretation of the partition function for colloidal clusters, *Physical Review E* **98**, 032608 (2018), 1806.00155.
  - [14] A. Murugan, J. Zou, and M. P. Brenner, Undesired usage and the robust self-assembly of heterogeneous structures, *Nature Communications* **6**, 6203 (2015).
  - [15] J. Bohlin, A. J. Turberfield, A. A. Louis, and P. Sulc, Designing the Self-Assembly of Arbitrary Shapes Using Minimal Complexity Building Blocks, *ACS Nano* **17**, 5387 (2023), 2207.06954.
  - [16] M. Grünwald and P. L. Geissler, Patterns without Patches: Hierarchical Self-Assembly of Complex Structures from Simple Building Blocks, *ACS Nano* **8**, 5891 (2014).
  - [17] O. G. Hayes, B. E. Partridge, and C. A. Mirkin, Encoding hierarchical assembly pathways of proteins with DNA, *Proceedings of the National Academy of Sciences* **118**, e2106808118 (2021).
  - [18] A. Murugan, Z. Zeravcic, M. P. Brenner, and S. Leibler, Multifarious assembly mixtures: Systems allowing retrieval of diverse stored structures, *Proceedings of the National Academy of Sciences* **112**, 54 (2015), 1408.6893.

- [19] P. Sartori and S. Leibler, Lessons from equilibrium statistical physics regarding the assembly of protein complexes, *Proceedings of the National Academy of Sciences* **117**, 114 (2020).
- [20] S. Osat and R. Golestanian, Non-reciprocal multifarious self-organization, *Nature Nanotechnology* **18**, 79 (2023).
- [21] C. Sigl, E. M. Willner, W. Engelen, J. A. Kretzmann, K. Sachenbacher, A. Liedl, F. Kolbe, F. Wilsch, S. A. Aghvami, U. Protzer, M. F. Hagan, S. Fraden, and H. Dietz, Programmable icosahedral shell system for virus trapping, *Nature Materials* **20**, 1281 (2021).
- [22] D. Hayakawa, T. E. Videbaek, D. M. Hall, H. Fang, C. Sigl, E. Feigl, H. Dietz, S. Fraden, M. F. Hagan, G. M. Grason, and W. B. Rogers, Geometrically programmed self-limited assembly of tubules using DNA origami colloids, *Proceedings of the National Academy of Sciences* **119**, e2207902119 (2022), 2203.01421.
- [23] T. E. Videbæk, H. Fang, D. Hayakawa, B. Tyukodi, M. F. Hagan, and W. B. Rogers, Tiling a tubule: how increasing complexity improves the yield of self-limited assembly, *Journal of Physics: Condensed Matter* **34**, 134003 (2022), 2111.04717.
- [24] T. E. Videbæk, D. Hayakawa, G. M. Grason, M. F. Hagan, S. Fraden, and W. B. Rogers, Economical routes to size-specific assembly of self-closing structures, *arXiv* 10.48550/arxiv.2311.01383 (2023), 2311.01383.
- [25] S. H. Park, C. Pistol, S. J. Ahn, J. H. Reif, A. R. Lebeck, C. Dwyer, and T. H. LaBean, Finite-Size, Fully Addressable DNA Tile Lattices Formed by Hierarchical Assembly Procedures, *Angewandte Chemie* **118**, 6759 (2006).
- [26] P.-S. Huang, S. E. Boyken, and D. Baker, The coming of age of de novo protein design, *Nature* **537**, 320 (2016).
- [27] S. E. Boyken, Z. Chen, B. Groves, R. A. Langan, G. Oberdorfer, A. Ford, J. M. Gilmore, C. Xu, F. DiMaio, J. H. Pereira, B. Sankaran, G. Seelig, P. H. Zwart, and D. Baker, De novo design of protein homo-oligomers with modular hydrogen-bond network-mediated specificity, *Science* **352**, 680 (2016).
- [28] D. Avis and K. Fukuda, Reverse search for enumeration, *Discrete Applied Mathematics* **65**, 21 (1996).
- [29] D. Avis and C. Jordan, mts: a light framework for parallelizing tree search codes, *Optimization Methods and Software* **36**, 279 (2021).
- [30] D. Avis and C. Jordan, mpls: A scalable parallel vertex/facet enumeration code, *Mathematical Programming Computation* **10**, 267 (2018).
- [31] L. Babai and E. M. Luks, Canonical labeling of graphs, *Proceedings of the fifteenth annual ACM symposium on Theory of computing - STOC '83*, 171 (1983).
- [32] B. D. McKay and A. Piperno, Practical graph isomorphism, II, *Journal of Symbolic Computation* **60**, 94 (2014).
- [33] In principle, *nauty* could be replaced by a more specialized, polynomial-time algorithm [32, 43–45] since all graphs we encounter here are of bounded degree, or even planar for two-dimensional structures.
- [34] M. C. Hübl and C. P. Goodrich, Roly.jl: Reverse-search polyform enumerator, <https://github.com/mxhbl/Roly.jl> (2024).
- [35] G. Caporossi and P. Hansen, Enumeration of Polyhex Hydrocarbons to  $h = 21$ , *Journal of Chemical Information and Computer Sciences* **38**, 610 (1998).
- [36] X. Liang, R. Wang, and J. x. Meng, Code for polyomino and computer search of isospectral polyominoes, *Journal of Combinatorial Optimization* **33**, 254 (2017).
- [37] For the structures considered here, this search took on the order of hours on a 2019 MacBook Pro.
- [38] S. E. Ahnert, I. G. Johnston, T. M. A. Fink, J. P. K. Doye, and A. A. Louis, Self-assembly, modularity, and physical complexity, *Physical Review E* **82**, 026117 (2010), 0912.3464.
- [39] A. Trubiano and M. Holmes-Cerfon, Thermodynamic stability versus kinetic accessibility: Pareto fronts for programmable self-assembly, *Soft Matter* **17**, 6797 (2021).
- [40] M. R. Perkett and M. F. Hagan, Using Markov state models to study self-assembly, *The Journal of Chemical Physics* **140**, 214101 (2014), 1402.1784.
- [41] F. M. Gartner, I. R. Graf, and E. Frey, The time complexity of self-assembly, *Proceedings of the National Academy of Sciences* **119**, e2116373119 (2022).
- [42] F. M. Gartner and E. Frey, Design Principles for Fast and Efficient Self-Assembly Processes, *Physical Review X* **14**, 021004 (2024).
- [43] E. M. Luks, Isomorphism of graphs of bounded valence can be tested in polynomial time, *Journal of Computer and System Sciences* **25**, 42 (1982).
- [44] J. E. Hopcroft and J. K. Wong, Linear time algorithm for isomorphism of planar graphs (Preliminary Report), *Proceedings of the sixth annual ACM symposium on Theory of computing - STOC '74*, 172 (1974).
- [45] C. J. Colbourn and K. S. Booth, Linear Time Automorphism Algorithms for Trees, Interval Graphs, and Planar Graphs, *SIAM Journal on Computing* **10**, 203 (1981).